Global NEST Journal, **28** (3), 07828
Available online: 28/04/2026

Multi-Index Assessment of Hydrometeorological Droughts in Northeast Algeria: Sectoral K-means Analysis of Trends and Water Resource Impacts

Amina Amarchi[1], Lotfi Zeghadnia[2]*, Moncef Chabi[1] and Hocine Amarchi[1]

[1]Laboratory of Soil and Hydraulic, Department of Hydraulic, Faculty of Technology, Badji Mokhtar Annaba University, Annaba, 23000, Algeria.
[2]Professor, Laboratory of Modeling and Socio-Economic Analysis in Water Science "MASESE", University of Souk Ahras, 41000, Algeria.

*Correspondence e-mail: lotfi.zeghadnia@univ-soukahras.dz

Abstract

Drought poses significant challenges to water availability, agriculture, and socioeconomic stability in Northeast Algeria. This study delineates the region into North (Mediterranean), Center (semi-arid), and South (arid) sectors using K-Means clustering and assesses drought trends with SPI, RDI, and SDI from 1975–2021. Results indicate near-normal conditions in the North (SPI-mean = 0.00023, RDI-mean = 0.003), transitional drying in the Center (SPI-mean = 0.0007, RDI-mean = 0.0008), and severe aridification in the South (SPI-mean = -0.0004, RDI-mean = -0.0007). Significant drying trends were observed in Oum El Bouaghi ($Z = -8.620$, $p < 0.0001$) and Khenchela ($Z = -6.357$, $p < 0.0001$). SDI analysis revealed stable streamflow but short-term drought risks at Medjaz Amar and Zerdaza Dam. Strong correlations among indices, particularly RDI with SPI and SDI, highlight the South's heightened vulnerability. These findings provide critical insights for policymakers to develop targeted drought mitigation strategies, such as enhanced water storage and efficient irrigation systems.

Keywords: Drought indices, Trend Analysis, Sectoral K-means, Northeast Algeria, Water resource management.

OPEN ACCESS

Received: 09/07/2025,

Accepted: 18/04/2026,

Available online: 28/04/2026

Copyright: © 2026 Global NEST. This article is an open access article distributed under the terms and conditions of the Creative Commons Attribution International (CC BY 4.0) license.

Graphical abstract

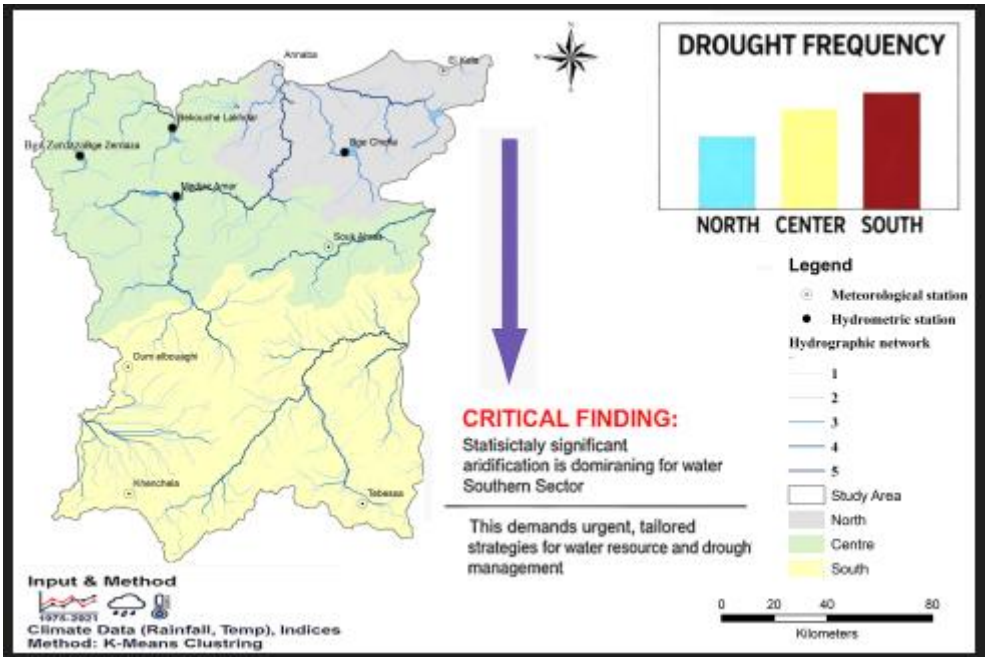

1. Introduction

Climate change, particularly drought, is projected to drive significant internal migration worldwide. According to a World Bank report (Clement *et al.*, 2021), climate-induced droughts could displace over 216 million people by 2050, affecting approximately 3% of the global population across regions such as East Asia, South Asia, Eastern Europe, North Africa, Sub-Saharan Africa, and Latin America. In Algeria, this projection is particularly alarming, with forecasts indicating a 10-20% decline in precipitation and temperature increases of up to 7°C in summer and 4°C in winter by mid-century. With an arid to semi-arid climate and increasing urbanization, the country faces heightened risks of recurrent droughts, floods, and escalating water demands. Algeria is already experiencing intensifying droughts, exacerbating desertification, soil salinization, and surface water degradation, leading to irregular rainfall patterns, declining streamflow, and extreme hydrological events (Guebail *et al.*, 2017). The National Economic and Social Council (CNES) reports that Algeria ranks among the world's most water-stressed nations, with an average annual per capita water availability of only 500 m³, far below the World Bank's water scarcity threshold of 1000 m³ (Hallouz *et al.*, 2024). Given this critical context, accurate drought assessment tools are essential for diagnosing drought behavior and supporting sustainable water resource planning. The Mediterranean Basin, particularly North Africa, is a climate change "hotspot" where drought impacts are projected to intensify (Giorgi & Lionello., 2008). Standardized drought indices such as the Standardized Precipitation Index (SPI), Reconnaissance Drought Index (RDI), and Streamflow Drought Index (SDI) are widely used to monitor meteorological and hydrological droughts. The SPI, developed by McKee *et al.* (1993, 1995), is valued for its flexibility and minimal data requirements. The RDI, which incorporates potential evapotranspiration (Tsakiris & Vangelis., 2005), is particularly suitable for semi-arid and arid climates like Algeria. The SDI, proposed by Nalbantis (2009), extends analysis to streamflow-based droughts, linking climatic and hydrological processes. These indices provide complementary insights into drought severity, duration, and spatial extent, enabling effective monitoring and mitigation strategies (Hayes, 2000). Drought assessment in the Maghreb and Mediterranean regions has been extensively studied using SPI, RDI, and SDI, with a focus on their applicability to diverse climatic conditions. In Morocco, Ouatiki *et al.* (2019) analyzed rainfall trends from 1970–2010 using SPI, revealing increasing drought frequency in semi-arid basins, consistent with patterns observed in Northeast Algeria. Similarly, Meliho *et al.* (2020) identified relationships between meteorological and agricultural droughts in Morocco's Tensift Watershed by comparing SPI at multiple timescales with water allocations for major crops, highlighting the agricultural impacts of drought. Aghrab *et al.* (2008) used SPI to compare drought patterns in Meknes, Morocco, and Córdoba, Spain, noting frequent early-season droughts and decreasing severity with increasing extremity, suggesting recurrent drought risks. In Tunisia, Merabti *et al.* (2018) compared SPI and RDI from 1958–2020, finding that RDI is more sensitive to evapotranspiration in arid settings, with SPI showing an increasing trend and RDI indicating a decreasing trend in northern Tunisia. Across the broader Mediterranean, Vicente-Serrano *et al.* (2017) used SPI to study drought variability, projecting intensified drought risks due to precipitation declines. In Italy, Marini *et al.* (2019) applied SPI and RDI in the Apulia region, confirming

their reliability for assessing meteorological droughts, while Vergoni *et al.* (2021) integrated SPI, RDI, SPEI, and SDDI to evaluate sunflower crop yields in central Italy from 1980–2019, demonstrating the value of multi-index approaches for agricultural impacts. In Turkey, Gumus and Algin (2017) established reliable relationships between meteorological (SPI) and hydrological (SDI) droughts in the Seyhan–Ceyhan Basins, emphasizing the importance of integrating both indices for comprehensive drought analysis. Another study in Turkey (source not specified) analyzed spatiotemporal variations in meteorological drought using SPI-3, SPI-6, and SPI-12, identifying regional differences in drought intensity. In Algeria, drought research has expanded over the past two decades. Bendjema *et al.* (2019) used SPI and SDI in the Mellah Catchment, reporting recurrent moderate to severe droughts. Haied *et al.* (2023) assessed drought hazards across three climatic zones, noting elevated risks in semi-arid regions, while Bouguerra *et al.* (2024) observed a shift from near-normal to moderately dry conditions in northern Algeria using SPI and SPEI. Choutri and Hussien (2024) highlighted persistent negative drought trends across all timescales, and Derradji *et al.* (2023) used spatio-temporal remote sensing to reveal heterogeneous drought intensities across northern, central, and southern regions. Lazri *et al.* (2015) confirmed an increasing probability of extreme drought events, aligning with observed hydrological stress. Amarchi *et al.* (2025) and Khoualdia *et al.* (2023) emphasized the need for multi-index integration to improve trend detection and water management reliability. Despite the abundance of regional drought research, major gaps remain in Algeria's drought assessment framework. Most existing studies focus solely on precipitation-based indices (SPI, RDI) and overlook streamflow-derived metrics such as SDI, which are crucial for understanding hydrological responses. Furthermore, few studies apply unsupervised classification methods like K-means clustering to objectively define homogeneous drought zones while reducing spatial bias from geographic coordinates. Consequently, spatial differentiation of drought intensity across Northeast Algeria remains poorly understood, especially when comparing climatic and hydrological signals.

This study addresses these research gaps by integrating SPI, RDI, and SDI indices over a long-term period (1975–2021) using data from multiple meteorological and hydrometric stations. Through the application of K-means clustering, the region is objectively divided into three climatic sectors-North (Mediterranean), Center (semi-arid transitional), and South (arid). Non-parametric trend analyses (Kruskal–Wallis, Mann–Kendall, and Theil–Sen), complemented by False Discovery Rate (FDR) correction, ensure robust detection of drought trends. This multi-index, sectoral approach provides a comprehensive diagnostic of drought severity and persistence, contributing to evidence-based water management and adaptation strategies for one of Algeria's most vulnerable regions.

2. Material and Methods

2.1. *Study Area Description and Location*

The study area in eastern Algeria spans Mediterranean (north), semi-arid (center), and arid (south) zones, from the Mediterranean coast to the Sahara (**Figure 1**). It includes eight wilayas, with 5.4 million people (38% rural) in 2020. The north has forests and moderate climate, while the south features plateaus and arid conditions. Precipitation ranges from 200 mm (south) to 1500 mm (north); temperatures vary from 1°C–15°C (winter) to 25°C–46°C (summer). Water resources (308 million m^3/year) support agriculture and livestock.

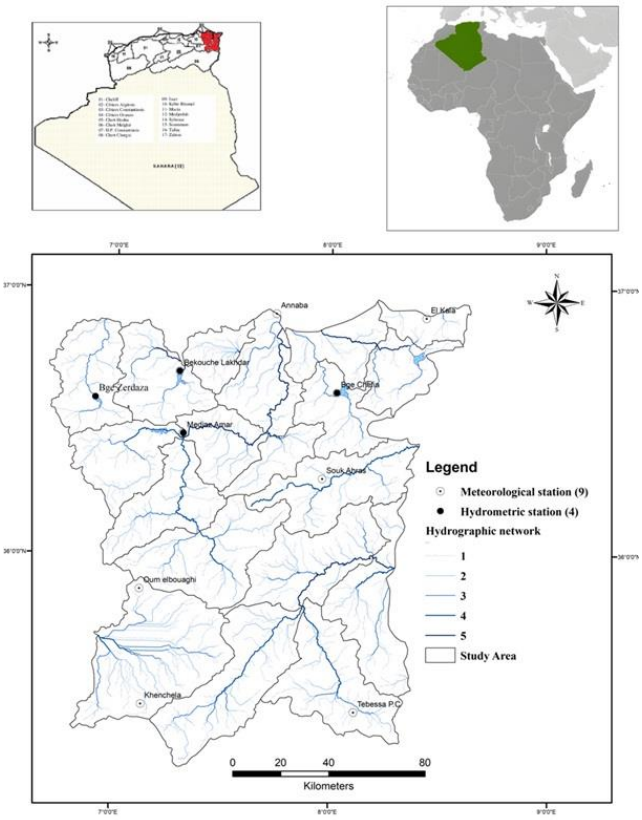

Figure 1. Geographical location of the study area.

2.2. *Data Collection*

In this stage, essential climatic and hydrological data were gathered to support the study. Precipitation data were obtained from ten (10) meteorological stations (see **Table 1**) strategically distributed across the three climatic zones of the study region: Mediterranean in the north, semi-arid in the center, and arid in the south, ensuring comprehensive regional coverage.

The precipitation data were sourced from the National Agency of Hydraulic Resources (ANRH), dam monitoring stations, and the hydraulic department of Skikda wilaya, covering the hydrological period from 1975 to 2021. Additionally, temperature data were collected from eight (08) sites, while river flow data were compiled for the same time span, providing a robust dataset for analyzing long-term climatic variability and hydrological trends in the region.

2.2.1. K-Means Clustering

K-means clustering was applied to classify meteorological stations into three sectors (North, Center, South) based on a combination of variables: mean SPI and RDI values

(amplified with weights of 0.4 each) and geographic coordinates (X, Y; minimized with weights of 0.1 each) to prioritize climatic indices over spatial location. All variables were standardized (z-score scaling) to ensure equal contribution. The optimal number of clusters (K=3) was validated using the elbow method, where the within-cluster sum of squares (WSS) plot showed a clear "elbow" at K=3, and silhouette scores averaged 0.65, indicating good cluster separation.

Table 1. List of stations used in the study.

Watershed	Stations	Wilaya	Coordinates	
			X (km)	Y (km)
Seybouse	Annaba	Annaba	951.1000	411.3500
	Medjez Amar	Guelma	907.2298	360.4421
Constantinois Center (East)	El kalla	El Taref	1012.3078	415.0438
	Chafia Dam	El Taref	977.1500	381.3000
Constantinois Center (West)	Zardaza Dam	Skikda	875.3000	374.6000
	Bekouche Lakhdar	Skikda	898.9990	386.2050
Madjerda-Mellague	Souk Ahras	Souk Ahras	971.2980	343.7510
	Tebessa	Tebessa	991.9000	247.2000
Constantinois High Plains watershed	Oum Elbouaghi	Oum Elbouaghi	898.2859	293.5758
	Khenchela	Khenchela	903.9185	249.4205

2.3. *Statistical Analysis of the Data*

The reliability and accuracy of statistical analysis are directly dependent on data quality. High-quality and complete datasets enable the correct identification of trends, cycles, and anomalies, ensuring the robust application of statistical methods and enhancing confidence in the findings. To achieve these, various statistical tests were conducted as follows:

Quality control procedures included checking for missing values (imputed using linear interpolation for < 5% gaps), outliers (removed if > 3 standard deviations from mean), and data consistency via cross-validation with nearby stations. Homogeneity was further assessed as below (McKee *et al.*, 1993; Tsakiris *et al.*, 2007).

2.3.1. Homogeneity Analysis

Homogeneity testing is crucial for analyzing categorical data across groups to detect significant differences (Dodge., 2008). Methods include statistical tests, graphical, and spectral analyses, chosen based on data and objectives. Parametric tests assume normal distribution and homogeneous variances, fitting interval/ratio data. Non-parametric tests, distribution-free, suit non-normal data.

2.3.2. Normality Testing

Testing for normality is a crucial step in determining whether parametric tests can be applied or if non-parametric methods should be used instead. Several statistical tests are widely utilized for this purpose, including Shapiro-Wilk test, Kolmogorov-Smirnov test and Anderson-Darling test (Nestel *et al.*, 2019; Dodge., 2008).

2.3.3. Kolmogorov-Smirnov Test

Introduced by Kolmogorov (1933) and formalized by Smirnov (1948), the Kolmogorov-Smirnov test evaluates if a dataset matches a specified distribution, often used for normality checks. The test statistic is:

$$D = max\,|F_n(x) - F(x.\mu.\sigma)| \quad (1)$$

$$D_{n.n} = \sqrt{n}.D \quad (2)$$

Where $F_n(x)$ is the empirical distribution function and $F(x.\mu.\sigma)$ is the theoretical cumulative distribution function. D is the maximum difference between the empirical distribution function $F_n(x)$ and the theoretical cumulative distribution function $F(x.\mu.\sigma)$, $D_{n.n}$ is the normalized test statistic, where "n" is the sample size. Large values of "D" suggest that the data do not follow a normal distribution. When the population parameters "μ" and "σ" are unknown sample estimates are used instead of the parameter values. (Kolmogorov., 1933), (Dodge., 2008).

2.3.4. Shapiro-Wilk test

The Shapiro-Wilk test, developed by Shapiro and Wilk (1965), is a widely used normality test. Its statistic W is calculated as:

$$W = \left(\sum_{i=1}^{n} a_i x_{(i)}\right)^2 / \sum_{i-1}^{n} (x_i - \bar{x})^2 \quad (3)$$

Where: x_i are the ordered sample values, $\bar{x}$ is the sample mean, and a_i are constants derived from the sample size. A small W indicates non-normality (Shapiro and Francia, 1972; Weisberg and Bingham, 1975; Royston, 1982).

Non-parametric tests, like the Kruskal-Wallis test, do not assume normality and are ideal for small samples or datasets with outliers, effectively assessing differences between multiple independent groups.

2.3.5. Kruskal-Wallis Test

The Kruskal-Wallis test (Kruskal and Wallis, 1952) is a non-parametric test to assess significant differences among three or more independent groups on a non-normally distributed continuous variable. It ranks all data values (smallest = 1, next = 2, etc.), calculates rank sums (R_i) for each group (i = 1, 2, ..., k) with sample size n_i, and computes the test statistic H, adjusted for ties:

$$H = \left(12/N(N+1)\right)\sum_{i=1}^{k}\frac{R_i^2}{n_i} - 3(N+1).\ N = \sum_{i=1}^{k} n_i \quad (4)$$

where:

- N is the total sample size across all groups computed as $N = \sum n_i$.

H follows a chi-square (χ^2) distribution with (k - 1) degrees of freedom (Van, 2010). A p-value < 0.05 rejects the null hypothesis, indicating at least one group differs significantly. It's ideal when parametric test assumptions (e.g., ANOVA) are violated

2.4. *Advanced Analysis: Non-Homogeneous Data*

When a non-parametric test indicates that a dataset is not homogeneous, it suggests the presence of significant differences between compared groups. In such cases, post-hoc tests are necessary to determine which groups exhibit these differences. Commonly used post-hoc tests include Dunn's test, Nemenyi's test, Conover's test, and van der Waerden's test, each of which identifies specific group differences and aids in refining further statistical analysis. Additionally, segmenting the dataset into homogeneous parts allows for more precise analysis and interpretation (Agbangba *et al.*, 2024; Nestel *et al.*, 2019).

2.4.1. Dunn's Post-hoc Test

The Dunn test (Dunn, 1964) is a non-parametric post-hoc test used after a Kruskal-Wallis test to detect specific group differences by comparing rank sums between pairs, adjusting for multiple comparisons. The Conover-Iman test (Conover, 1979) is a more powerful variant (Nestel *et al.*, 2019). Dunn's test statistic (Q) is calculated as:

$$Q = \left(R_i - R_j\right) / \sqrt{\frac{N(N+1)}{12}\sum\left(\frac{1}{n_i} + \frac{1}{n_j}\right)} \quad (5)$$

Where R_i and R_j are the rank sums for groups i and j. N is the total number of observations and n_i and n_j are the sample sizes of the groups. The test result yields p-values which are compared against a significance level (α = 0.05). If the p-value is below α the difference between the compared groups is considered statistically significant (Dinno., 2015; Dunn., 1961-1964; Glantz., 2012).

2.5. *Overview of Drought Indices*

Drought, a major natural disaster, causes significant socio-economic and environmental damage, contributing to ~22% of global economic losses from natural disasters (Karbasi *et al.*, 2023; Malik *et al.*, 2021). Its severity, location, duration, and timing are assessed using climatic or hydrometeorological indices (WMO, 2016).

2.5.1. Standardized Precipitation Index (SPI)

Drought, a major natural disaster, causes 22% of global economic losses (Malik *et al.*, 2021). Defined by severity, location, duration, and timing, it is monitored using climatic or hydrometeorological indices (WMO, 2016). Regional assessments use meteorological station data, with methodologies like the SPI employing single or multiple indices for enhanced accuracy and prediction:

$$SPI = \left(P_{ij} - \overline{PX}\right) / \sigma \quad (6)$$

Where: Pij represents seasonal precipitation at the i[th] gauge and j[th] observation $\overline{P}$: denotes the long-term seasonal mean, and σ stands for the standard deviation.

The SPI quantifies precipitation anomalies to identify dry and wet periods. Drought occurs when SPI values stay below -1 for consecutive periods and ends when positive. Severity is classified using SPI thresholds (Tsakiris and Vangelis., 2004) (**Table 2**).

2.5.2. Reconnaissance Drought Index (RDI)

The Reconnaissance Drought Index (RDI) assesses drought using precipitation and potential evapotranspiration (PET) for accurate water deficit evaluation (Tsakiris and Vangelis, 2005). RDI provides a comprehensive drought representation, effective across diverse climates, and is more sensitive to environmental changes than SPI (Tigkas *et al.*, 2015). It is calculated as initial value (α_k), normalized RDI (RDI_n), and standardized RDI (RDI_{st}):

$$\propto_k^i = \sum_{j=1}^{k} P_{ij} / \sum_{j=1}^{k} PET_{ij},\ \ i = 1(1)N\ \ et\ j = 1(1)k \quad (7)$$

Where P_{ij} and PET_{ij} are the precipitation and potential evapotranspiration for month j of hydrological year i.

The values of α_k typically follow log-normal or gamma distributions across various locations and time scales. For a log-normal distribution, the standardized RDI (RDI_{st}) can be calculated using:

$$RDI_{st}^{(i)} = \left(y^{(i)} - \overline{y}\right) / \hat{\sigma}_y \quad (8)$$

Where $y^{(i)}$ is $\left(\propto_k^i\right)$, $\overline{y_k}$ is its arithmetic mean, and $\hat{\sigma}_y$ is its standard deviation.

Positive RDI_n values indicate wet periods; negative values signify dry periods relative to normal conditions. Drought severity is classified as mild, moderate, severe, or extreme based on RDI thresholds (**Table 2**).

2.5.3. Streamflow Drought Index (SDI)

The Streamflow Drought Index (SDI) (Nalbantis *et al.*, 2009) assesses hydrological drought using normalized monthly streamflow to identify wet/dry periods and drought intensity. Suitable for station-based monitoring but may not reflect entire basins. SDI is calculated as:

$$V_{i.k} = \sum_{j=1}^{3k} Q_{ij} ..\ i = 1.\ 2,\ j = 1.2.....12.\ k = 1.\ 2.\ 3.4 \quad (9)$$

Where:

$V_{i.k}$: is the cumulative flow of hydrological year (i) for reference period (k).

K = 1 for October-December, K = 2 for October-March, K = 3 for October-June, and K = 4 for October-September.

Using the calculated cumulative streamflows, the SDI for each reference period k is determined as:

$$SDI_{i.k} = \left(V_{i.k-\overline{Vk}}\right) / S_k . i = 1.2..... K = 1.\ 2.\ 3.4 \quad (10)$$

Where:

V_k and S_k are the mean and standard deviation respectively of cumulative flows for reference period k calculated over a long period.

The SDI classification, akin to the SPI, defines five hydrological drought severity levels (**Table 2**). It evaluates long-term water availability, assesses watershed drought response, and supports water resource management.

Table 2. Summary of dry and wet categories from various drought indices based on the index value (Gulmez *et al.*, 2021). (Tigkas., 2015).

Categories	Meteorological and Hydrological Drought. SPI. RDI and SDI
Extremely Dry	≤ -2
Severe Dry	[-1.5: -2]
Moderately Dry	[-1: -1.5]
Near Normal	[-1 : 1]
Moderately Wet	[1: 1.5]
Very Wet	[1.5: 2]
Extremely Wet	≥+2

2.6. *Trends Analysis*

2.6.1. Mann-Kendall Analysis and Theil-Sen Estimator

The Mann-Kendall (MK) test, developed by Mann (1945) and refined by Kendall (1975), is a non-parametric method to detect monotonic trends in time series data, commonly used in hydrological and meteorological studies (Tuan *et al.*, 2021). The test statistic (S) is calculated as described:

$$S = \sum_{i=1}^{N-1} \sum_{j=i+1}^{N} sgn\left(x_j - x_i\right) \quad (11)$$

And

$$sgn\left(x_j - x_i\right) = \begin{Bmatrix} +1 & if\left(x_j - x_i\right) > 0 \\ 0 & if\left(x_j - x_i\right) = 0 \\ -1 & if\left(x_j - x_i\right) < 0 \end{Bmatrix} \quad (12)$$

Therefore, S > 0 indicates an upward trend, while S < 0 indicates a downward trend; Moreover, for a more accurate result and assessment it is necessary to calculate the variance (VAR) (Helsel and Hirsch., 1992). VAR is computed using the following equation:

$$VAR(S) = \frac{1}{18}\left[n(n-1)(2n+5) - \sum_{p=1}^{g} t_p \left(t_p - 1\right)\left(2t_p + 5\right) \right] \quad (13)$$

Where: *tp* represents the number of ties in the sample p, and g denotes the number of groups with the same data values. If *VAR* (*S*) > 0, the trend is positive; if *VAR* (*S*) < 0, the trend is negative. The Mann-Kendall Z statistic is then determined as:

$$\begin{aligned} Z &= (S-1)/\left[VAR(S)\right]^{1/2} \quad S > 0 \\ Z &= 0 \quad S = 0 \\ Z &= (S+1)/\left[VAR(S)\right]^{1/2} \quad S < 0 \end{aligned} \quad (14)$$

If $Z > 0$, it indicates an upward trend; if $Z < 0$, a downward trend.

2.6.2. Modified Mann-Kendall (Wang, 2004)

Autocorrelation in time series data invalidates the Mann-Kendall test by violating its assumption of independent observations, reducing effective sample size and risking misleading trend significance inferences.

2.6.3. The Yue and Wang (2004) Adjustment

Yue and Wang (2004) proposed a refined version of the Mann-Kendall test designed to address serial correlation in time series data by adjusting the variance to reflect the effective sample size. The modified variance is:

$$Var^*(S) = \left(n / n^*\right) Var(S) \quad (15)$$

where n^* is the effective sample size. It is defined by:

$$\left(n / n^*\right) = 1 + \frac{2}{n} \sum_{K=1}^{n-1} (n-k)\rho(k) \quad (16)$$

and ρ(k) denotes the autocorrelation at lag k. The revised test statistic is:

$$Z^* = (S \pm 1)/\left[VAR(S)\right]^{1/2} (or\ 0\ if\ S = 0) \quad (17)$$

To account for multiple testing across stations, timescales, and indices (total of 120 tests), False Discovery Rate (FDR) correction using the Benjamini-Hochberg (Benjamini and Hochberg, 1995) procedure was applied (α = 0.05). Unlike the conservative Bonferroni method, which divides α by the number of tests and controls family-wise error rate, the FDR approach controls the expected proportion of false positives among all rejected null hypotheses. This adaptive threshold increases detection power for true trends while preserving statistical validity, making it particularly suitable for exploratory trend analysis in hydroclimatic studies. Only p-values below their rank-specific FDR threshold were considered significant.

2.6.4. Theil-Sen Estimator

The Theil-Sen estimator, introduced by Theil (1950) and refined by Sen (1968), is a non-parametric method for estimating linear trends in time series data, robust against outliers (Kocsis *et al.*, 2020). The Theil-Sen slope (Q) is calculated as:

$$Q = \left(x_j^{`} - x_i\right) / \left(t_j - t_i\right) \quad (18)$$

where x_j, x_i are data values at times t_i, t_j respectively. The overall trend is then estimated as the median of all calculated slopes:

$$Sen's\ slope = median(Q) \quad (19)$$

The trend estimate, resilient to outliers, monitors hydrometeorological data changes (Kocsis *et al.*, 2020). SPSS, DrinC (Tigkas *et al.*, 2015), ProUCL 5.2.0 (USEPA, 2022), and Python (Carricano *et al.*, 2010; Kocsis *et al.*, 2020) enabled efficient computation, drought trend detection, and visualization for robust statistical validation

3. Results and discussion

3.1. *Reliability of the Data*

High-quality data is essential for robust statistical analysis. Normality test results for rainfall, temperature, and streamflow data in Northeast Algeria, presented in **Table 3**, consistently indicate non-normal distributions. For rainfall, Kolmogorov-Smirnov (KS) statistics range from 0.143 to 0.189 and Shapiro-Wilk (SW) statistics from 0.786 to 0.867, with p-values of 0.000, rejecting the null hypothesis of normality. Temperature data similarly show non-normality, with KS statistics of 0.143–0.189, SW statistics of 0.786–0.867, and p-values of 0.000. Streamflow data exhibit even greater deviation, with KS statistics of 0.254–0.313, SW statistics of 0.506–0.697, and p-values of 0.000, confirming non-normality. These findings, summarized in **Table 3**, necessitate the use of non-parametric methods for reliable trend analysis.

3.1.1. Non-Parametric Test

Non-parametric methods are required for trend analysis in Northeast Algeria, as rainfall, temperature, and streamflow data exhibit non-normal distributions, as confirmed by normality tests (**Table 3**). **Table 4** presents Kruskal-Wallis test results for rainfall, showing no significant differences across stations (p-values: Annaba: 1.000, Zerdaza Dam: 0.997, Bekouche Lakhdar: 0.966, Chafia Dam: 0.999, Medjaz Amar: 0.986, El Kala: 1.000, Khenchela: 0.489, Oum El Bouaghi: 0.266, Souk Ahras: 0.985, Tebessa: 0.190; all > 0.05). H statistics (16.329–54.206, 46 df) confirm similar rainfall distributions, supporting the use of non-parametric methods for hydrological trend analysis.

For temperature, the Kruskal-Wallis test (**Table 4**) indicates consistent distributions across most stations (p-values: Annaba: 1.000, H = 8.047; Zerdaza Dam: 1.000, H = 9.123; Bekouche Lakhdar: 1.000, H = 59.171; Medjaz Amar: 1.000, H = 15.962; El Kala: 1.000, H = 8.892; Khenchela: 1.000, H = 8.144; Oum El Bouaghi: 1.000, H = 21.635; Souk Ahras: 0.999, H = 9.078; Tebessa: 1.000, H = 9.563). Chafia Dam shows a slightly lower p-value (0.092, H = 9.094), suggesting minor distributional differences, though not statistically significant.

Table 3. Normality Test Results for Rainfall, Temperature, and Streamflow Data

Stations	Kolmogorov-Smirnov (KS) *Statistic*			Shapiro-Wilk (SW) *Statistic*			*P-value*
	Rainfall Data	Temperature Data	Streamflow Data	Rainfall Data	Temperature Data	Streamflow Data	
Annaba	0.163	0.106		0.867	0.938		0.000
Zerdaza Dam	0.166	0.097	0.254	0.834	0.959	0.697	0.000
BekoucheLakhdar	0.189	0.106	0.308	0.819	0.945	0.552	0.000
Chafia Dam	0.155	0.082	0.313	0.866	0.973	0.526	0.000
Medjaz Amar	0.164	0.107	0.313	0.838	0.938	0.506	0.000
El kalla	0.171	0.098		0.841	0.956		0.000
Khenchela	0.179	0.102		0.786	0.936		0.000
Oum El Bouaghi	0.158	0.107		0.819	0.938		0.000
Souk Ahras	0.162	0.092		0.830	0.952		0.000
Tebessa	0.143	0.107		0.853	0.933		0.000

Table 4. Kruskal-Wallis Non-Parametric Test Results for Rainfall, Temperature, and Streamflow Data.

Stations	*Kruskal-Wallis H*			*P-Value*		
	Rainfall Data	Temperature Data	Streamflow Data	Rainfall Data	Temperature Data	Streamflow Data
Annaba	19.219	8.047		1.000	1.000	
Zerdaza Dam	23.975	9.123	236.29	0.997	1.000	0.000
Bekouche Lakhdar	30.092	59.171	137.997	0.966	1.000	0.000
Chafia Dam	22.431	9.094	82.067	0.999	0.092	0.01
Medjaz Amar	27.455	15.962	117.542	0.986	1.000	0.001
El kalla	16.329	8.892		1.000	1.000	
Khenchela	45.598	8.144		0.489	1.000	
Oum El Bouaghi	51.546	21.635		0.266	1.000	
Souk Ahras	27.650	9.078		0.985	0.999	
Tebessa	54.206	9.563		0.190	1.000	

Streamflow data analysis via the Kruskal-Wallis test (**Table 4**) reveals significant variability, with H statistics ranging from 82.067 to 236.29. Significant differences are observed at Zerdaza Dam (p = 0.000, H = 236.29), Bekouche Lakhdar (p = 0.000, H = 137.997), Chafia Dam (p = 0.01, H = 82.067), and Medjaz Amar (p = 0.001, H = 117.542), where p-values < 0.05 reject the null hypothesis of similar distributions. Streamflow data were not available for Annaba, El Kala, Khenchela, Oum El Bouaghi, Souk Ahras, and Tebessa, limiting analysis to the four listed stations. These results highlight streamflow heterogeneity, necessitating non-parametric methods for assessing hydrological variability in the region.

3.2. *Advanced Analysis: Segmentation and Post-Hoc Testing.*

Streamflow data exhibits significant heterogeneity (**Table 7**), necessitating advanced pairwise comparison techniques. Segmentation into 46 homogeneous groups (46 years), as shown in **Figures 2–5**, enables precise hydrological trend analysis, with Dunn's post-hoc test clarifying group differences.

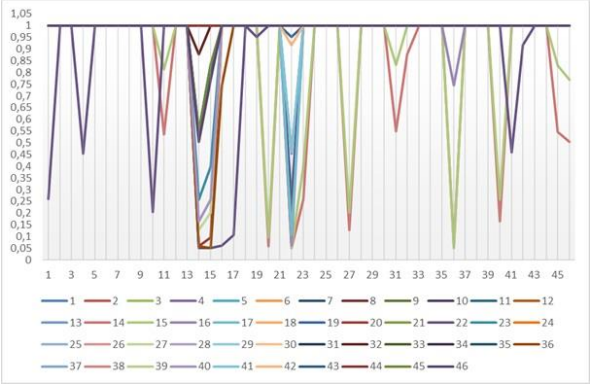

Figure 2. Dunn's Post-Hoc Test Results for Medjaz Amar Station Streamflow.

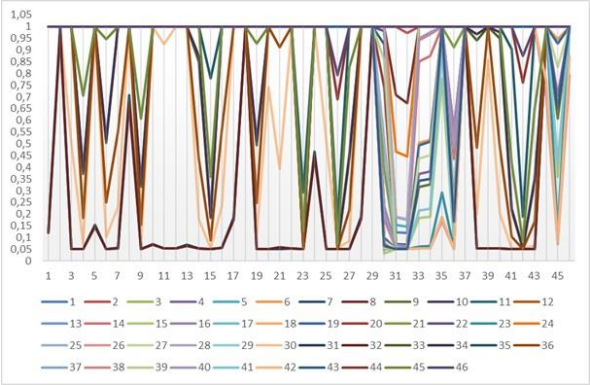

Figure 3. Dunn's Post Hoc Test Results for Zerdaza Dam Station Streamflow.

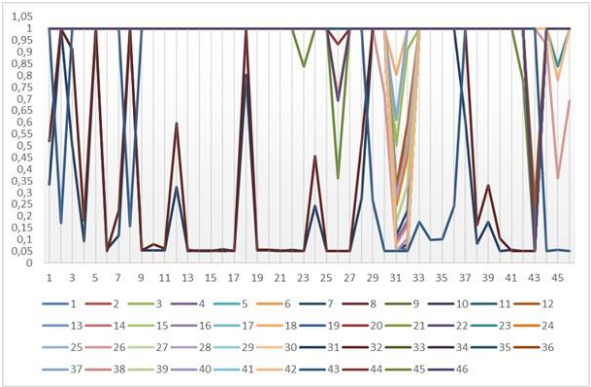

Figure 4. Dunn's Post Hoc Test Results for Bekouch Lakhdar Station Streamflow.

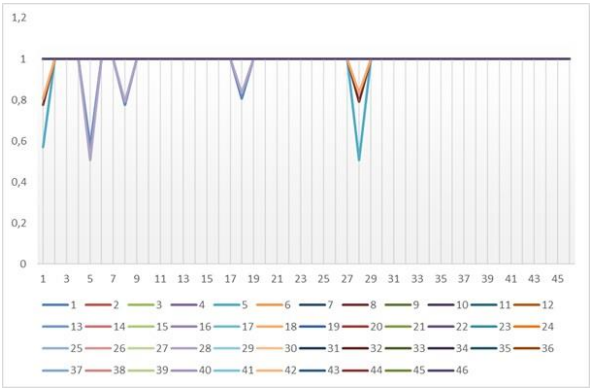

Figure 5. Dunn's Post Hoc Test Results for Chafia Dam Station Streamflow.

Streamflow patterns at Medjaz Amar, Zerdaza Dam, and Bekouche Lakhdar are similar, with Dunn's test p-values ~0.05, showing marginal but not significant differences. Chafia Dam's p-values >0.4 confirm no significant variations. Regional hydrological consistency suggests common drivers, supporting reliable assessments (**Figures 2, 3, 4**).

3.3. *Drought Indices analysis*

3.3.1. K-Means Clustering and Drought Trend Analysis for Meteorological Station Classification

3.2.1.1 K-Means Clustering for Geo-Climatic Sector Classification

Meteorological stations were classified into North, Center, and South sectors using K-Means clustering based on latitude (Y-coordinates), reflecting the hypothesis that proximity to the Mediterranean Sea corresponds to a wetter Mediterranean climate, while greater distance inland leads to drier, more arid conditions. The 10-station dataset was objectively grouped into three clusters: stations with the highest Y-coordinates (North, closest to the Mediterranean), intermediate Y-coordinates (Center, semi-arid transitional zone), and lowest Y-coordinates (South, arid interior) (**Figure 6**). The validity of this classification was confirmed through Mann-Kendall trend analyses of Hydrometeorological indices.

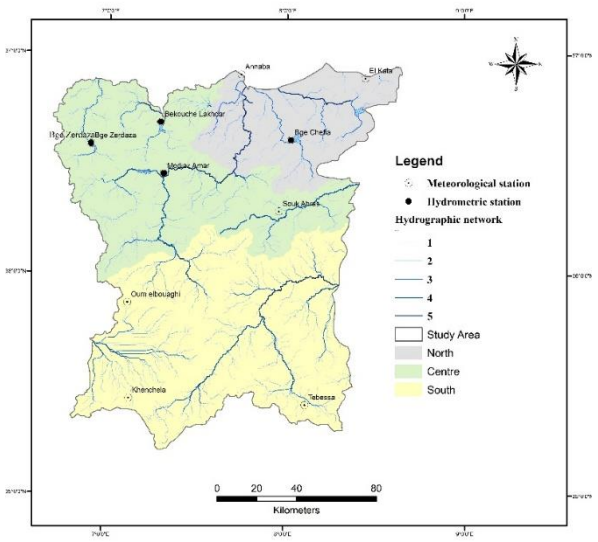

Figure 6. Climatic Sector Classification Based on K-Means Clustering.

3.3.2. Statistical Validation with SPI and RDI Trends

The Mann-Kendall test confirmed that the geographical classification captures climatic patterns, leveraging SPI 12 and RDI 12 for drought trend analysis, with a strong emphasis on minimizing the influence of geographic coordinates (X, Y) and amplifying the role of SPI and RDI indices. Mean values (**Table 5**) reveal the North as humid (SPI-mean = 0.00023, RDI-mean = 0.003), the Center as a transitional zone (SPI-mean = 0.0007, RDI-mean = 0.0008), and the South as drier (SPI-mean = -0.0004, RDI-mean = -0.0007).

Table 5. Mann-Kendall Test Results for SPI and RDI Trends Across Climatic Sectors.

Station	X	Y	SPI-mean	SPI-std	SPI-mean-Cluster	RDI-mean	RDI-std	RDI-mean-Cluster
Annaba	951.1	411.35	0.000301	1.011137	0.00023	0.000527	1.011146	0.003
El Kala	1012.31	415.04	-10^{-4}	1.011104		0.000465	1.011136	
Chafia Dam	977.15	381.3	0.000482	1.011161		0.00741	1.012468	
Zerdaza Dam	875.3	374.6	$-4.1.10^{-5}$	1.011089	0.0007	-0.00017	1.011088	0.0008
Bekouche Lakhdar	899	386.2	0.001351	1.011278		0.001469	1.01129	
Medjaz Amar	907.23	360.44	0.00112	1.011214		0.001437	1.011243	
Souk Ahras	971.3	343.75	0.00031	1.01113		0.00035	1.011133	
Oum El Bouaghi	898.29	293.58	$-6.1.10^{-5}$	1.011097	-0.0004	-0.00042	1.011052	-0.0007
Khenchela	903.92	249.42	-0.00011	1.011102		-0.00069	1.011025	
Tebessa	991.9	247.2	-0.00098	1.011003		-0.00108	1.010988	

Table 6. Kruskal-Wallis Test Results for SPI and RDI Means Across Climatic Sectors.

Index	Statistic (H-value)	P-value
SPI-mean	5.50	0.064
RDI-mean	5.98	0.050

Kruskal-Wallis tests found no significant differences among sectors, supporting their grouping into North, Center, and South (**Table 6**). This validates SPI and RDI as reliable indicators of sectors' climatic characteristics.

Figure 7 boxplots of SPI-mean and RDI-mean show positive values in the humid North, near-zero in the balanced Center, and negative in the dry, water-stressed South, confirming the utility of integrating climatic indices, statistical tests, and visualizations for enhanced classification (**Figure 7**).

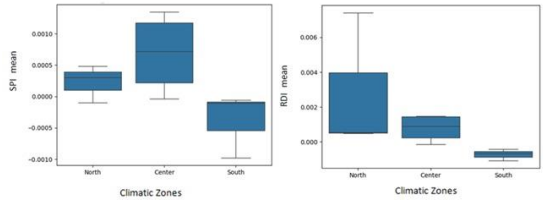

Figure 7. Distribution of SPI-mean and RDI-mean Across Climatic Zones (North, Center, and South).

3.2.2.1 Northern Sector

The multi-panel visualization of SPI and RDI for Algeria's northern sector indicates a gradual increase in drought severity, with SPI-12 and RDI-12 panels showing persistent negative trends for prolonged dry conditions. Shorter timescales (SPI-01, RDI-01, SPI-03, RDI-03) reveal variability, suggesting occasional dry spells or rare wet events. Annaba, Chafia Dam, and El Kala highlight a regional drying trend, likely worsened by the shift from Mediterranean to semi-arid climates, underscoring the need for adaptive water management (**Figure 8**).

3.2.2.2 Center Sector

The treemap highlights increasing drought in center sector, where SPI06, RDI06, and 12-month indices dominate—signaling prolonged dryness. Souk Ahras shows mainly short-term variability (SPI01, RDI01). Medjaz Ammar's wider range, including SPI03 and RDI03, reflects a fragile and unstable climate. SPI and RDI analyses for Constantinois Center (West) and North Medjerda–Mellague/Central Sybous watersheds indicate a growing drought trend in northern Algeria, with near normal to

moderate dry periods and a slow, persistent drying in the Medjerda–Mellague region.

3.2.2.3 Southern Sector

The treemap (**Figure 10**) highlights sustained dryness in the southern side of the study area, covering the northern Constantinois High Plains and the southern Medjerda–Mellague watershed (via Tebessa station). Khenchela, Oum El Bouaghi, and Tebessa show dominant SPI06, RDI06, and SPI12 values, indicating prolonged dry conditions. Short-term indices (SPI01, RDI01) are less frequent, reinforcing a trend of long-lasting water stress. The scarcity of extreme wet events reflects a stable but increasingly arid climate across this southern zone.

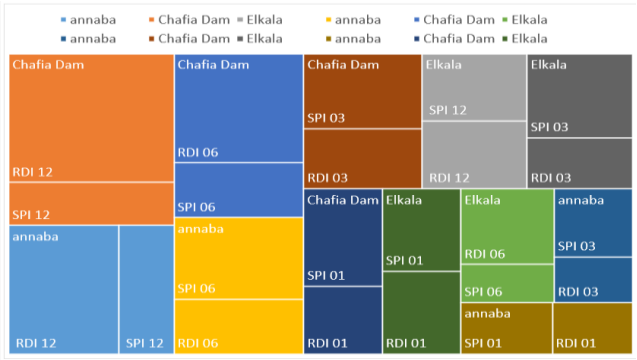

Figure 8. Multi-Timescale SPI and RDI Analysis of Drought Trends in Northern Algeria (Sybous Watershed and Constantinois-East).

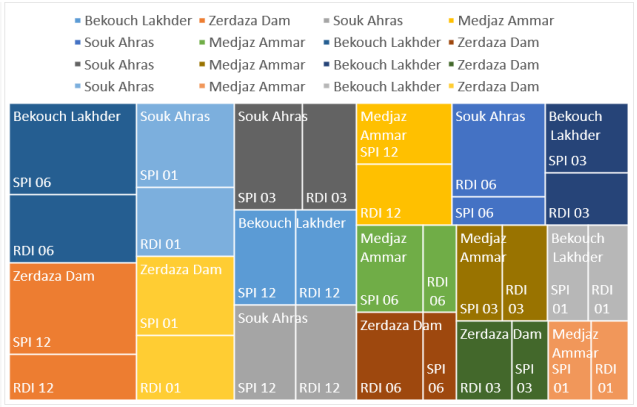

Figure 9. SPI and RDI in the Constantinois Center (West), North Medjerda–Mellague, and Central Sybous Watersheds (Northeast Algeria).

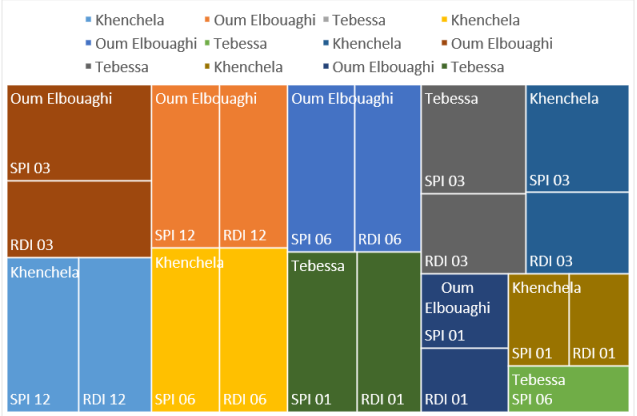

Figure 10. Drought Patterns in Southern Constantinois and Medjerda–Mellague Watersheds (Tebessa Region).

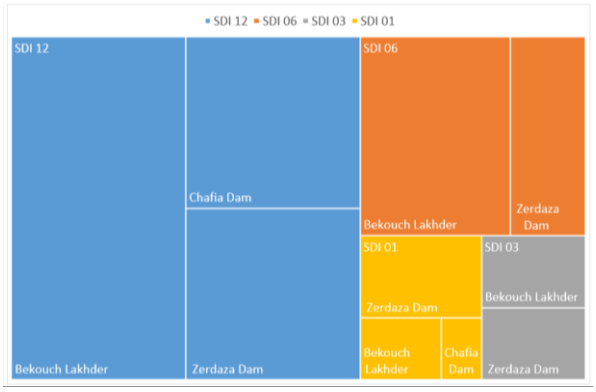

Figure 11. Multi-Timescale SDI Analysis of Drought Severity in Northern Algeria.

3.4. *Streamflow Drought Index (SDI)*

The Dunn test finds homogeneity only for annual data (46 years), supporting reliable yearly analysis for the study area (Dunn, 1964). Shorter periods remain key for detecting seasonal drought variations.

The multi-panel SDI (**Figure 11**) visualization for northern Algeria's stations (Bekouch Lakhdar, Chafia Dam, Zerdaza Dam) highlights a regional drying trend across timescales (SDI-12, SDI-06, SDI-03, SDI-01). Chafia Dam shows mostly near-normal conditions with occasional short-term droughts (SDI-01, SDI-03) and rare severe droughts, indicating periodic dryness and vulnerability, supported by homogeneous data but variable climatic influences (Constantinois East watershed). Medjaz Amar, Bekouch Lakhdar, and Zerdaza Dam also exhibit near-normal conditions, though short-term indices (SDI-01, SDI-03) reveal emerging drought trends, with Medjaz Amar experiencing frequent moderate to severe droughts and rare extreme events, signaling heightened hydrological stress.

3.4.1. Spatiotemporal Analysis of Drought indices

Multi-index drought analysis using SPI, RDI, and SDI at 12-month timescale (**Figures 12–14**) reveals recurrent and spatially heterogeneous drought episodes across the study area from 1975 to 2021. Severe meteorological and hydrological droughts are consistently identified in 1987–1988, 1996–1997, 2001–2002, and 2015–2016, with SPI and RDI dropping below −2.0 in multiple stations, and SDI reaching −2.2 at Bekouche Lakhdar in 1996–1997 and −2.3 at Chafia Dam in 2001–2002, confirming extreme streamflow deficits (Haied *et al.*, 2023; Bedjema *et al.*, 2019).Northern stations (Annaba, El Kala, Chafia Dam) exhibit sharp SPI and RDI minima in 1996–1997 (SPI < −2.0 at Annaba and El Kala) and 2001–2002 (RDI < −2.4 at Annaba), reflecting intense precipitation and evaporative stress (Ziari & Medjerab., 2024). In contrast, central dams (Zerdaza Dam, Bekouche Lakhdar) show SDI as the most sensitive indicator, recording −2.2 in 1996–1997 and −1.6 in 2015–2016, highlighting prolonged hydrological drought despite moderate meteorological signals (Haied *et al.*, 2023). Southern stations (Khenchela, Oum El Bouaghi, Tebessa) display amplified RDI deficits in 2007–2008 (RDI ≈ −2.2 at Khenchela and Oum El Bouaghi) and 2015–2016, driven by high evapotranspiration under warming

conditions, with SPI and RDI converging toward −1.5 to −2.0, indicating progressive aridification (Khoualdia *et al.*, 2023; Rabah & Mohamed., 2025).The SDI uniquely captures downstream propagation of drought, with delayed and amplified responses in reservoir inflows (e.g., 1987–1990, 2016–2017), underscoring its critical role in water resource risk assessment. These results emphasize the complementarity of SPI, RDI, and SDI in revealing regional drought dynamics and sector-specific vulnerabilities.

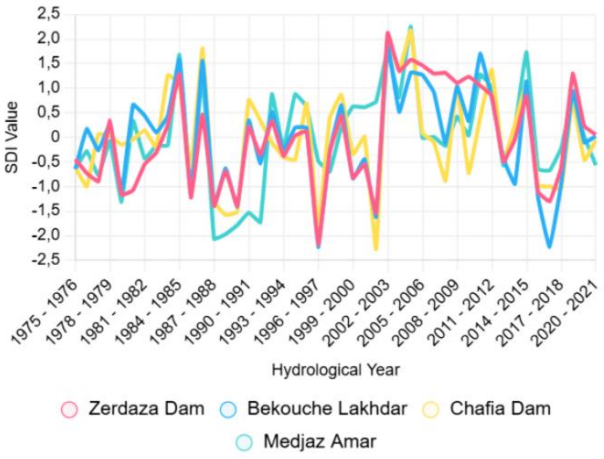

Figure 12. Variation of SDI (12-Month Timescale) Across Key Stations in the Study Area.

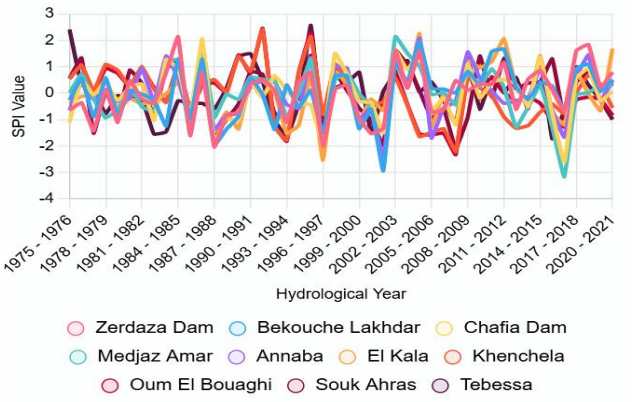

Figure 13. Temporal Patterns of SPI (12-Month Timescale) for Stations in the Study Area.

3.5. *Trends analysis*

3.5.1. Northern Sector

The Modified Mann-Kendall test with FDR correction (α = 0.05; critical threshold p ≤ 0.0104) reveals widespread drying in the Northern study area. Short-term drought is evident with significant trends in SPI 1 at Annaba (p = 0.0018) and El Kala (p = 0.00), RDI 1 at Annaba (p = 0.0083) and El Kala (p = 0.00), and Chafia Dam's SDI 1 (Z = -6.503, p = 0.00), confirming severe short-term drought. Medium-term indices (SPI 3, RDI 3, SPI 6) at Annaba and El Kala, and SDI 3 at Chafia Dam (p = 0.00), also indicate drying. Long-term SPI 12 at El Kala (p = 0.0001) shows pronounced drying, while Annaba's SPI 12 (p = 0.1015) is non-significant after FDR. These trends urge adaptive water management to address intensifying drought conditions.

Table 7. The Modified Mann-Kendall Results for SPI. RDI. and SDI Indices in the Northern Study Area Watersheds.

Station	Indices	Original MK	Original MK Z	Modified MK Z (Wang)	P-value (Original)	P-value (Modified)	S (Test Statistic)	Sen's Slope	Significant after FDR (Modified, $\alpha = 0.05$)
Annaba	SPI 1	0.023	0.795	3.12	0.427	0.0018	3440	0.0002	Yes
	RDI 1	0.016	0.565	2.639	0.572	0.0083	2446	0.0001	Yes
	SPI 3	0.051	1.033	3.117	0.302	0.0018	864	0.0014	Yes
	RDI 3	0.039	0.779	2.647	0.436	0.0081	652	0.001	Yes
	SPI 6	0.034	0.476	1.454	0.634	0.146	142	0.002	No
	RDI 6	0.002	0.024	0.074	0.981	0.9411	8	0.0002	No
	SPI 12	0.038	0.36	1.638	0.719	0.1015	39	0.0029	No
	RDI 12	-0.024	-0.227	-0.903	0.82	0.3667	-25	-0.0021	No
Chafia Dam	SPI 1	-0.028	-0.993	-2.956	0.321	0.0031	-4301	-0.0002	Yes
	RDI 1	-0.002	-0.064	-0.17	0.949	0.8649	-278	0	No
	SDI 1	-0.114	-3.987	-6.503	0	0	-17260	-0.0011	Yes
	SPI 3	-0.001	-0.013	-0.06	0.989	0.9523	-12	0	No
	RDI 3	0.027	0.547	1.373	0.584	0.1698	458	0.0008	No
	SDI 3	-0.089	-1.786	-4.448	0.074	0	-1493	-0.0025	Yes
	SPI 6	0.003	0.037	0.163	0.97	0.8705	12	0.0004	No
	RDI 6	0.023	0.32	0.578	0.749	0.5635	96	0.0014	No
	SDI 6	0.004	0.051	0.127	0.96	0.8991	16	0.0003	No
	SPI 12	0.036	0.341	1.395	0.733	0.1631	37	0.0047	No
	RDI 12	-0.009	-0.076	-0.128	0.94	0.8982	-9	-0.0009	No
	SDI 12	0.02	0.189	0.552	0.85	0.5808	21	0.0021	No
El kalla	SPI 1	0.051	1.793	4.328	0.073	0	7764	0.0004	Yes
	RDI 1	0.051	1.793	4.328	0.073	0	7764	0.0004	Yes
	SPI 3	0.089	1.786	4.43	0.074	0	1493	0.0026	Yes
	RDI 3	0.087	1.743	4.1	0.081	0	1457	0.0024	Yes

	SPI 6	0.108	1.514	3.532	0.13	0.0004	450	0.0058	Yes
	RDI 6	0.075	1.056	2.561	0.291	0.0104	314	0.0046	Yes
	SPI 12	0.152	1.477	4.038	0.14	0.0001	157	0.0195	Yes
	RDI 12	0.08	0.776	2.058	0.438	0.0396	83	0.0103	No

3.5.2. Center of the area study

Table 8 presents Modified Mann-Kendall results with FDR correction (α = 0.05; critical threshold p ≤ 0.0245). Bekouch Lakhdar shows significant drying in SPI 1, 3, 6, 12; RDI 1, 3, 6, 12; and SDI 3. Zerdaza Dam exhibits stronger trends across SPI 1, 3, 6, 12; RDI 3, 6, 12; and SDI 1, 3, 6, 12. Medjaz Amar reveals significant drying in SDI 1, 3, 6, 12 and wetting in RDI 1, 6, 12. Souk-Ahras remains stable (all p > 0.114). Bekouch Lakhdar and Zerdaza Dam face highest drought risk, necessitating targeted water management.

3.5.3. Southern Sector

Table 9 presents Modified Mann-Kendall results with FDR correction (α = 0.05; critical threshold p ≤ 0.0269). Khenchela and Oum Elbouaghi show significant drying in RDI 1, SPI 3, RDI 3, SPI 6, RDI 6, SPI 12, and RDI 12 (p ≤ 0.0156). Tebessa exhibits no significant trends after FDR (highest p = 0.0299 > 0.0288). Khenchela and Oum Elbouaghi face highest drought risk, necessitating targeted water management.

Table 8. The Modified Mann-Kendall Test Results for SPI. RDI. and SDI Indices Across Stations in the Center of the area study.

Station	Indices	Original MK	Original MK Z	Modified MK Z (Wang)	P-value (Original)	P-value (Modified)	S (Test Statistic)	Sen's Slope	Significant after FDR (Modified, α=0.05)
Bekouch Lakhdar	SPI 1	0.071	2.492	4.141	0.013	0	10788	0.0006	Yes
	RDI 1	0.063	2.192	3.65	0.028	0.0003	9491	0.0005	Yes
	SDI 1	0.069	2.414	1.822	0.016	0.0685	10450	0.0006	No
	SPI 3	0.136	2.745	5.534	0.006	0	2294	0.0037	Yes
	RDI 3	0.122	2.458	4.978	0.014	0	2054	0.0035	Yes
	SDI 3	0.088	1.773	2.25	0.076	0.0245	1482	0.0024	Yes
	SPI 6	0.151	2.128	3.935	0.033	0.0001	632	0.0087	Yes
	RDI 6	0.106	1.494	2.824	0.135	0.0047	444	0.0065	Yes
	SDI 6	0.053	0.745	1.389	0.456	0.1649	222	0.0036	No
	SPI 12	0.206	2.007	4.499	0.045	0	213	0.0192	Yes
	RDI 12	0.15	1.458	3.576	0.145	0.0003	155	0.0145	Yes
	SDI 12	0.043	0.417	0.992	0.677	0.3213	45	0.0061	No
Zerdaza Dam	SPI 1	0.031	1.079	2.85	0.281	0.0044	4672	0.0003	Yes
	RDI 1	0.021	0.723	1.84	0.469	0.0657	3132	0.0002	No
	SDI 1	0.187	6.577	4.103	0	0	28471	0.0017	Yes
	SPI 3	0.09	1.82	4.656	0.069	0	1521	0.0026	Yes
	RDI 3	0.068	1.377	3.681	0.169	0.0002	1151	0.002	Yes
	SDI 3	0.211	4.245	4.431	0	0	3547	0.006	Yes
	SPI 6	0.154	2.169	5.392	0.03	0	644	0.0087	Yes
	RDI 6	0.118	1.663	4.26	0.096	0	494	0.0063	Yes
	SDI 6	0.208	2.931	4.091	0.003	0	870	0.0111	Yes
	SPI 12	0.243	2.367	7.019	0.018	0	251	0.0243	Yes
	RDI 12	0.144	1.401	3.64	0.161	0.0003	149	0.0172	Yes
	SDI 12	0.186	1.818	3.304	0.069	0.001	193	0.0246	Yes
Souk-Ahras	SPI 1	0.006	0.222	0.764	0.824	0.4448	964	0.0001	No
	RDI 1	-0.004	-0.155	-0.385	0.876	0.7	-674	0	No
	SPI 3	0.02	0.408	1.193	0.683	0.2329	342	0.0006	No
	RDI 3	0.011	0.219	0.494	0.827	0.621	184	0.0004	No
	SPI 6	0.041	0.577	1.247	0.564	0.2124	172	0.0029	No
	RDI 6	0.047	0.664	1.2	0.506	0.23	198	0.0031	No
	SPI 12	0.057	0.549	1.581	0.583	0.114	59	0.0055	No
	RDI 12	0.038	0.36	0.836	0.719	0.403	39	0.006	No
Medjaz Amar	SPI 1	-0.025	-0.868	-1.91	0.385	0.0562	-3759	-0.0002	No
	RDI 1	-0.032	-1.137	-2.704	0.255	0.0068	-4924	-0.0003	Yes
	SDI 1	0.125	4.399	2.813	0	0.0049	19043	0.0009	Yes
	SPI 3	-0.013	-0.253	-0.654	0.801	0.5132	-212	-0.0004	No
	RDI 3	-0.025	-0.496	-1.34	0.62	0.1804	-415	-0.0007	No
	SDI 3	0.14	2.823	3.011	0.005	0.0026	2359	0.0029	Yes

	SPI 6	-0.019	-0.266	-0.728	0.79	0.4669	-80	-0.0009	No
	RDI 6	-0.07	-0.981	-2.794	0.326	0.0052	-292	-0.004	Yes
	SDI 6	0.163	2.304	3.184	0.021	0.0015	684	0.009	Yes
	SPI 12	-0.007	-0.057	-0.128	0.955	0.8979	-7	-0.0005	No
	RDI 12	-0.115	-1.117	-2.658	0.264	0.0079	-119	-0.0143	Yes
	SDI 12	0.185	1.799	3.274	0.072	0.0011	191	0.0201	Yes

The FDR-corrected Modified Mann-Kendall analysis (Benjamini-Hochberg procedure at $\alpha = 0.05$) controls the false discovery rate across sector-specific tests (Northern: 24 tests, threshold $p \leq 0.0104$; Center: 20 tests, $p \leq 0.0245$; Southern: 18 tests, $p \leq 0.0269$), minimizing Type I errors in this heterogeneous dataset. It reveals a stark north-to-south drought intensification gradient, with significant drying trends (p below sector thresholds) widespread in the North (e.g., SPI-1 at Annaba: $p = 0.0018$; El Kala: $p < 0.001$; SDI-1 at Chafia Dam: $p < 0.001$, $Z = -6.503$), concentrated in the Center (e.g., Bekouche Lakhdar: significant across SPI-1/3/6/12, RDI-1/3/6/12, SDI-3; Zerdaza Dam: SPI-1/3/6/12, RDI-3/6/12, SDI-1/3/6/12), and most pronounced in the South (e.g., Khenchela: SPI-12 $Z = -6.357$, slope = -0.0294, $p < 0.001$; RDI-12 $Z = -8.233$, slope = -0.0378, $p < 0.001$; Oum El Bouaghi: SPI-12 $Z = -8.620$, slope = -0.0298, $p < 0.001$; RDI-12 $Z = -12.500$, slope = -0.0371, $p < 0.001$; Tebessa: no significant trends, max $p = 0.0299 > 0.0269$). These reflect persistent aridification from declining precipitation and rising evapotranspiration, aligning with Mediterranean projections of 10 - 30% precipitation loss by 2050 (Giorgi & Lionello., 2008). Northern/central stations show more short/medium-term signals (e.g., SPI-3/6, SDI-3; 15–20% below thresholds), with emerging streamflow risks (SDI means ≈ -0.2 at Medjaz Amar), due to Mediterranean buffering.

Table 9. The Modified Mann-Kendall Test Results Highlighting Long-Term and Short-Term Drought Trends at Khenchela and Oum El Bouaghi Stations.

Station	Indices	Original MK	Original MK Z	Modified MK Z (Wang)	P-value (Original)	P-value (Modified)	S (Test Statistic)	Sen's Slope	Significant after FDR (Modified, α=0.05)
Khenchela	SPI 1	-0.022	-0.757	-1.636	0.449	0.1019	-3279	-0.0002	No
	RDI 1	-0.032	-1.109	-2.58	0.267	0.0099	-4803	-0.0003	Yes
	SPI 3	-0.066	-1.334	-3.556	0.182	0.0004	-1115	-0.0019	Yes
	RDI 3	-0.08	-1.61	-4.931	0.107	0	-1346	-0.0024	Yes
	SPI 6	-0.102	-1.44	-3.812	0.15	0.0001	-428	-0.0056	Yes
	RDI 6	-0.139	-1.96	-5.266	0.05	0	-582	-0.0084	Yes
	SPI 12	-0.293	-2.859	-6.357	0.004	0	-303	-0.0294	Yes
	RDI 12	-0.357	-3.484	-8.233	0	0	-369	-0.0378	Yes
Oum Elbouaghi	SPI 1	-0.012	-0.432	-1.097	0.666	0.2728	-1871	-0.0001	No
	RDI 1	-0.023	-0.822	-2.417	0.411	0.0156	-3561	-0.0002	Yes
	SPI 3	-0.068	-1.374	-4.276	0.169	0	-1149	-0.0019	Yes
	RDI 3	-0.084	-1.692	-6.145	0.091	0	-1414	-0.0023	Yes
	SPI 6	-0.12	-1.697	-5.909	0.09	0	-504	-0.0065	Yes
	RDI 6	-0.161	-2.277	-8.823	0.023	0	-676	-0.0084	Yes
	SPI 12	-0.298	-2.907	-8.62	0.004	0	-308	-0.0298	Yes
	RDI 12	-0.391	-3.825	-12.5	0	0	-405	-0.0371	Yes
Tebessa	SPI 1	0.02	0.715	1.533	0.474	0.1252	3098	0.0002	No
	RDI 1	0.008	0.264	0.66	0.792	0.509	1144	0.0001	No
	SPI 3	0.005	0.092	0.225	0.927	0.8218	78	0.0001	No
	RDI 3	-0.003	-0.056	-0.16	0.955	0.8731	-48	-0.0001	No
	SPI 6	0.008	0.111	0.32	0.911	0.7487	34	0.0007	No
	RDI 6	-0.034	-0.482	-1.454	0.63	0.146	-144	-0.0022	No
	SPI 12	0.007	0.057	0.18	0.955	0.8568	7	0.001	No
	RDI 12	-0.069	-0.663	-2.171	0.507	0.0299	-71	-0.0085	No

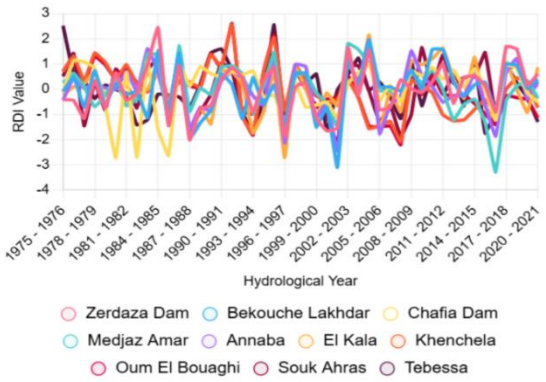

Figure 14. RDI (12-Month Timescale) Trends Across the Watersheds in the Study Area.

This FDR-validated detection of coherent drying patterns enhances trend attribution to climate forcing, though limitations include potential autocorrelations and station-data biases. For resilience, we recommend: (1) Southern rainwater harvesting and micro-catchments to boost recharge (20-30%; Guebail *et al.*, 2017; Loukas *et al.*, 2020) plus afforestation; (2) Central drought-tolerant crops and deficit irrigation to cut water use 15-25% while preserving yields (FAO, 2018; Haied *et al.*, 2023); (3) Northern reservoir enhancements at Zerdaza Dam via SDI forecasting and 10-15% capacity expansion. These evidence-based strategies, prioritized by FDR-confirmed severity, promote water security amid climatic stress in Northeast Algeria.

4. Conclusion

Drought threatens agriculture, water resources, food security, and socioeconomic stability in Northeast Algeria amid rising climate variability. This study integrates SPI, RDI, and SDI within a K-means-derived sectoral framework-prioritizing indices over geography to define North (Mediterranean), Center (semi-arid), and South (arid) zones. Non-parametric tests confirmed non-normal distributions, meteorological homogeneity (Kruskal-Wallis), and streamflow heterogeneity (Dunn's test identifying Medjaz Amar, Zerdaza Dam, and Bekouche Lakhdar as groups). FDR-corrected Modified Mann-Kendall and Theil-Sen analyses reveal a north-south drying gradient: near-normal North (SPI_mean = 0.00023, RDI_mean = 0.003) versus stressed Center and arid South (SPI_mean = -0.0004, RDI_mean = -0.0007), with severe trends at Oum El Bouaghi (SPI-12: $Z = -8.620$, $p < 0.0001$; RDI-12: $Z = -12.500$, $p < 0.0001$) and Khenchela (SPI-12: $Z = -6.357$, $p < 0.0001$; RDI-12: $Z = -8.233$, $p < 0.0001$). Short/medium-term signals (SPI 1-3, SDI3) prevail in North/Center, signaling risks, while long-term persistence amplifies Southern vulnerability. This multi-index approach validates sector-based monitoring for spatiotemporal insights, guiding resilience. Prioritize: Southern rainwater harvesting/afforestation for 20–30% recharge gains; Central drought-tolerant crops/deficit irrigation for 15–25% water savings; Northern Zerdaza Dam upgrades (10-15% expansion) via SDI forecasts. These strategies mitigate risks and ensure water security.

While the multi-index approach provides robust insights into drought dynamics, certain methodological constraints warrant consideration. The SDI analysis, based on only 4 dam stations (Zerdaza Dam, Bekouche Lakhdar, Chafia Dam, Medjaz Amar), is constrained by limited hydrometric data. This may underrepresent central hydrological trends, as ungauged areas could exhibit unrecorded drought severity, particularly given the absence of southern data. Consequently, SDI's non-significant trends (in Center) may underestimate risks compared to SPI/RDI, highlighting the need for expanded gauging networks. Future studies could integrate satellite-derived streamflow to mitigate this gap.

References

Agbangba, C. E., Aide, E. S., Honfo, H., & Kakai, R. G. (2024). On the use of post-hoc tests in environmental and biological sciences: A critical review. Heliyon, 10, e25131. https://doi.org/10.1016/j.heliyon.2024.e25131

Almedeij, J. (2014). Drought analysis for Kuwait using standardized precipitation index. The Scientific World Journal, 2014, 451841. https://doi.org/10.1155/2014/451841

Amarchi, A., Zeghadnia, L., Chabi, M., Amarchi, H., & Laouacheria, F. (2025). Enhancing drought trend analysis in northeastern Algeria with integrated classification frequencies for deeper insights. Modeling Earth Systems and Environment, 11, 328. https://doi.org/10.1007/s40808-024-02040-9

Benjamini, Y., & Hochberg, Y. (1995). Controlling the false discovery rate: A practical and powerful approach to multiple testing. Journal of the Royal Statistical Society: Series B (Methodological), 57(1), 289–300

Bendjema, L., Baba-Hamed, K., & Bouanani, A. (2019). Characterization of the climatic drought indices application to the Mellah catchment, North-East of Algeria. Journal of Water and Land Development, 43, 28–40. https://doi.org/10.2478/jwld-2019-0057

Bouguerra, H., Derdous, O., Tachi, S. E., Hatzaki, M., & Abida, H. (2024). Spatiotemporal investigation of meteorological drought variability over northern Algeria and its relationship with different atmospheric circulation patterns. Theoretical and Applied Climatology, 155, 1507–1518. https://doi.org/10.1007/s00704-023-04765-7

Buttafuoco, G., Caloiero, T., & Coscarelli, R. (2015). Analyses of drought events in Calabria (Southern Italy) using standardized precipitation index. Water Resources Management, 29, 557–573. https://doi.org/10.1007/s11269-014-0826-6

Carricano, M., Poujol, F., & Bertrandias, L. (2010). Analyse de données avec SPSS. Pearson Education.Choutri, I., & Hussien, A. (2024). Exploratory analysis of Algeria meteorological drought using SPI and SPEI. Open Access Library Journal, 11, e11897. https://doi.org/10.4236/oalib.1111897

Clement, V., Rigaud, K. K., De Sherbinin, A., Jones, B., Adamo, S., Schewe, J., & Shabahat, E. (2021). Groundswell Part 2: Acting on Internal Climate Migration. World Bank. https://doi.org/10.1596/36248

Conover, W. J., & Iman, R. L. (1979). Multiple-comparisons procedures (Rep. No. LA-7677-MS). Los Alamos National Laboratory.

Derradji, T., Belksier, M. S., Bouznad, I. E., Zebsa, R., Bengusmia, D., & Gastaldi, E. (2023). Spatio-temporal drought monitoring and detection of the areas most vulnerable to drought risk in Mediterranean region, based on remote sensing data (Northeastern Algeria). Arabian Journal of Geosciences, 16, 1. https://doi.org/10.1007/s12517-022-11207-3

Dinno, A. (2015). Nonparametric pairwise multiple comparisons in independent groups using Dunn's test. The Stata Journal, 15, 292–300. https://doi.org/10.1177/1536867X1501500117

Dodge, Y. (2008). The concise encyclopedia of statistics. Springer.Dunn, O. J. (1961). Multiple comparisons among means. Journal of the American Statistical Association, 56, 52–64. https://doi.org/10.1080/01621459.1961.10482090

Dunn, O. J. (1964). Multiple comparisons using rank sums. Technometrics, 6, 241–252. https://doi.org/10.1080/00401706.1964.10490181

FAO. (2018). The State of Food and Agriculture 2018: Migration, agriculture and rural development. Food and Agriculture Organization of the United Nations. http://www.fao.org/3/I9549EN/i9549en.pdf

Giorgi, F., & Lionello, P. (2008). Climate change projections for the Mediterranean region. Global and Planetary Change, 63, 90–104. https://doi.org/10.1016/j.gloplacha.2007.09.005

Glantz, S. A. (2012). Primer of biostatistics (7th ed.). McGraw Hill.

Guebail, A., Zeghadnia, L., Djebbar, Y., & Bouranene, S. (2017). Rainwater harvesting in Algeria: Utilization and assessment of the physico-chemical quality case study of Souk-Ahras region. Courrier du Savoir, 23, 85–94.

Gulmez, A., Mersin, D., Vaheddoost, B., & Safari, M. J. S. (2021). Evaluation of streamflow drought index in Aegean region, Turkey. In International Conference on Natural Resources and Sustainable Environmental Management (pp. 208–213). Springer. https://doi.org/10.1007/978-3-030-76320-6_23

Haied, N., Foufou, A., Khadri, S., Boussaid, A., Azlaoui, M., & Bougherira, N. (2023). Spatial and temporal assessment of drought hazard, vulnerability and risk in three different climatic zones in Algeria using two commonly used meteorological indices. Sustainability, 15, 7803. https://doi.org/10.3390/su15107803

Hallouz, F., Meddi, M., Ali Rahmani, S. E., & Abdi, I. (2024). Innovative versus traditional statistical methods in hydropluviometric: A detailed analysis of trends in the Wadi Mina Basin (Northwest of Algeria). Theoretical and Applied Climatology, 155, 8263–8286. https://doi.org/10.1007/s00704-024-04957-9

Hayes, M. J. (2000). Revisiting the SPI: Clarifying the process. Drought Network News, 12, 13–14.

Helsel, D. R., & Hirsch, R. M. (1992). Statistical methods in water resources. United States Geological Survey. https://doi.org/10.3133/tm4A3

Karbasi, M., Jamei, M., Malik, A., Kisi, O., & Yaseen, Z. M. (2023). Multi-steps drought forecasting in arid and humid climate environments: Development of integrative machine learning model. Agricultural Water Management, 281, 108210. https://doi.org/10.1016/j.agwat.2023.108210

Kendall, M. G. (1975). Rank correlation methods (4th ed.). Charles Griffin.Khoualdia, W., Derdous, O., Bouamrane, A., Abida, H., & Saber, M. (2023). Climate variability and its impact on water resources: Case study of the Souk Ahras region, northeastern Algeria. Desalination and Water Treatment, 296, 10–18. https://doi.org/10.5004/dwt.2023.29547

Kocsis, T., Kovács-Székely, I., & Anda, A. (2020). Homogeneity tests and non-parametric analyses of tendencies in precipitation time series in Keszthely, Western Hungary. Theoretical and Applied Climatology, 139, 849–859. https://doi.org/10.1007/s00704-019-02996-6

Kolmogorov, A. (1933). Sulla determinazione empirica di una legge di distribuzione. Giornale dell'Istituto Italiano degli Attuari, 4, 89–91.

Kruskal, W. H., & Wallis, W. A. (1952). Use of ranks in one-criterion variance analysis. Journal of the American Statistical Association, 47, 583–621. https://doi.org/10.1080/01621459.1952.10483441

Lazri, M., Ameur, S., Brucker, J. M., Lahdir, M., & Sehad, M. (2015). Analysis of drought areas in northern Algeria using Markov chains. Journal of Earth System Science, 124, 61–70. https://doi.org/10.1007/s12040-014-0532-7

Loukas, A., Mylopoulos, N., & Vasiliades, L. (2020). A GIS-based model for estimating the regional water balance in a semi-arid basin. Journal of Hydrology, 589, 125157. https://doi.org/10.1016/j.jhydrol.2020.125157

Malik, A., Tikhamarine, Y., Sammen, S. S., Abba, S. I., & Shahid, S. (2021). Prediction of meteorological drought by using hybrid support vector regression optimized with HHO versus PSO algorithms. Environmental Science and Pollution Research, 28, 39139–39158. https://doi.org/10.1007/s11356-021-13445-0

Mann, H. B. (1945). Non-parametric tests against trend. Econometrica, 13, 163–171. https://doi.org/10.2307/1907187

McKee, T. B., Doesken, N. J., & Kleist, J. (1993). The relationship of drought frequency and duration to time scales. In Proceedings of the 8th Conference on Applied Climatology (pp. 179–183). American Meteorological Society.

McKee, T. B., Doesken, N. J., & Kleist, J. (1995). Drought monitoring with multiple time scales. In Proceedings of the Ninth Conference on Applied Climatology (pp. 233–236). American Meteorological Society.

Merabti, A., Meddi, M., Martins, D. S., & Pereira, L. S. (2018). Comparing SPI and RDI applied at local scale as influenced by climate. Water Resources Management, 32, 1071–1085. https://doi.org/10.1007/s11269-017-1855-8

Nestel, D., Hui, J., Kunkler, K., Scerbo, M. W., & Calhoun, A. W. (2019). Developing expertise in healthcare simulation research. In Healthcare simulation research: A practical guide (pp. 3–7). Springer. https://doi.org/10.1007/978-3-030-26837-4_1

Ouatiki, H., Boudhar, A., Ouhinou, A., Arioua, A., Hssaisoune, M., Bouamri, H., & Benabdelouahab, T. (2019). Trend analysis of rainfall and drought over the Oum Er-Rbia River Basin in Morocco during 1970–2010. Arabian Journal of Geosciences, 12, 1. https://doi.org/10.1007/s12517-019-4238-6

Rabah, M., & Mohamed, T. H. (2025). Assessing drought dynamics in Northeastern Algeria using the vegetation health index derived from MODIS data. Carpathian Journal of Earth and Environmental Sciences, 20, 19–26. https://doi.org/10.26471/cjees/2025/020/001

Royston, J. P. (1982). An extension of Shapiro-Wilk's W test for non-normality to large samples. Applied Statistics, 31, 115–124. https://doi.org/10.2307/2347973

Sen, P. K. (1968). Estimates of the regression coefficient based on Kendall's tau. Journal of the American Statistical Association, 63, 1379–1389. https://doi.org/10.1080/01621459.1968.10480934

Shapiro, S. S., & Francia, R. S. (1972). An approximate analysis of variance test for normality. Journal of the American Statistical

Association, 67, 215–216. https://doi.org/10.1080/01621459.1972.10481232

Shapiro, S. S., & Wilk, M. B. (1965). An analysis of variance test for normality (complete samples). Biometrika, 52, 591–611. https://doi.org/10.1093/biomet/52.3-4.591

Simsek, O., Sankaran, A., & Şenol, H. İ. (2024). Multiscale investigations on RDI-SPI teleconnections of Çoruh and Aras Basins, Türkiye using time dependent intrinsic correlation. Physics and Chemistry of the Earth, Parts A/B/C, 136, 103787. https://doi.org/10.1016/j.pce.2024.103787

Tareke, K. A., & Awoke, A. G. (2022). Hydrological drought analysis using streamflow drought index (SDI) in Ethiopia. Advances in Meteorology, 2022, 7067951. https://doi.org/10.1155/2022/7067951

Tigkas, D., Vangelis, H., & Tsakiris, G. (2015). DrinC: A software for drought analysis based on drought indices. Earth Science Informatics, 8, 697–709. https://doi.org/10.1007/s12145-014-0178-y

Tsakiris, G., & Vangelis, H. (2004). Towards a drought watch system based on spatial SPI. Water Resources Management, 18, 1–12. https://doi.org/10.1023/B:WRAM.0000015410.47063.a4

Tsakiris, G., & Vangelis, H. (2005). Establishing a drought index incorporating evapotranspiration. European Water, 9/10, 3–11.

Tuan, N. H., & Canh, T. T. (2021). Analysis of trends in drought with the non-parametric approach in Vietnam: A case study in Ninh Thuan Province. American Journal of Climate Change, 10, 51–84. https://doi.org/10.4236/ajcc.2021.101004

United States Environmental Protection Agency. (2022). ProUCL: Statistical software for environmental applications for data sets with and without nondetect observations (Version 5.2). https://www.epa.gov/land-research/proucl-software

Van, H. T. (2010). Time series analysis to forecast temperature change. Mathematical Sciences, 35, 63–69.Weisberg, S., & Bingham, C. (1975). An approximate analysis of variance test for non-normality suitable for machine calculation. Technometrics, 17, 133–134. https://doi.org/10.1080/00401706.1975.10489281

Yue, S., & Wang, C. (2004). The Mann-Kendall test modified by effective sample size to detect trend in autocorrelated data. Water Resources Management, 18, 201–218. https://doi.org/10.1023/B:WRAM.0000043140.62684.1a

Ziari, A., & Medjerab, A. (2024). Impact of drought in Northeastern Algeria: Comparative study of the SPI and SPEI indices. Revista de Gestão Sociale Ambiental, 18, e06591. https://doi.org/10.24857/rgsa.v18n1-001